Supplementary Materials

Activin A directs porcine embryonic stem cell commitment to extraembryonic endoderm lineage

Hanning Wang[1,4*], Liang Zhong[3,4], Xiaofeng Yan[1], Kaipeng Wang[1], Chengchen Zhao[1], Jinzhu Xiang[1*], Duanqing Pei[1,2*]

[1]Laboratory of Cell Fate Control, School of Life Sciences, Westlake University, Hangzhou, 310030, China
[2]Westlake Laboratory of Life Sciences and Biomedicine, Hangzhou, 310030, China
L. Zhong
[3]Hebei Provincial Key Laboratory of Basic Medicine for Diabetes, The Shijiazhuang Second Hospital, Shijiazhuang, 050051, China
[4] These authors contributed equally to this work.
Corresponding authors:
peiduanqing@westlake.edu.cn; xiangjinzhu@westlake.edu.cn; wanghanning@westlake.edu.cn

Table S1. Primers for real-time quantitative PCR analyses in this study.

Gene	Forward (5'-3')	Reverse (5'-3')
EF1α	AATGCGGTGGGATCGACAAA	CACGCTCACGTTCAGCCTTT
POU5F1	TGAGGCTTTGCAGCTCAGTT	TCTCCAGGTTGCCTCTCACT
SOX2	CATCAACGGTACACTGCCTCTC	ACTCTCCTCCCATTTCCCTCTTT
NANOG	CCTACAATCCAGCTCTTTGG	CTCAGGCATTGGTGAAGATT
SOX17	CGCACGGAGTTTGAACAATA	CAGACGTCGGGGTAGTTACAG
GATA4	CGACACCCTAATCTCGATATGTTT	GTGGTGGTCTGGCAGTTGG
GATA6	ATCACCATCACCACCCAAGT	CGCGACTCTGTAGACTGTGC
COL4A1	GTGCATGCGGAGAACATGAC	AGGGTGTGTTAGTTACGCGG
PDGFRA	CAGGTTGGAGGGAGATGGAC	AGTTGCGGAGGTTGGATT
HNF4A	ACATGGACATGGCCGACTAC	GCACCTTCTGATGGGGATGT
APOE	GAAGATGAGGGTTCTGTGGGTT	TGGGTGACCTTGGTGCTGA
AFP	CACCTTTCCAGGTTCCAGAA	AAGGGGTGCCTTCTTGCTAT
PLAU	AAGGGCTCTGACATTCCATG	CCGGCTCTTACACTGACACA
CLDN6	CCTTCATCGGCAACAGCATC	GCCAGCAGCGAGTCATACACC
SPARC	GGACCATCAGTCCTCTGGAA	AGTTCTGCGTCTCCCAAAGA
VIM	GTACCGGAGACAGGTGCAGT	TTCCACGGCAAAGTTCTCTT
PAX6	CCGAATTCTGCAGACCCATG	TACTACCACCGATTGCCCTG
WNT1	TACTGCACGAGTGCCTGTGA	TCTTATGTGCCAGCGAACCT
PAX3	CGGGCTACAGTATGGACCCT	AGGGCCAGTTTAAGCTCCAAG

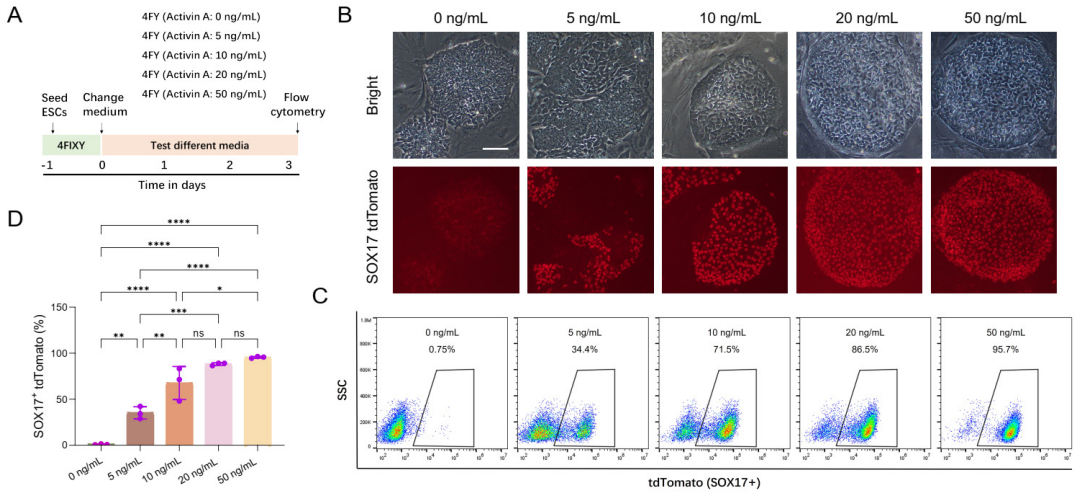


Figure S1. Activin A is required and concentration-dependent. A) Schematic of testing concentrations of Activin A during ESC-to-XEN cell transition. B) Morphology of cells treated by Activin A with various concentrations. Scale bar, 100 μm. C) The flow cytometric analysis of SOX17-positive cells. D) Bar chart showing the SOX17 positive cells quantified by flow cytometry analysis as in (C). The data are presented as the mean ± SD. n = 3. ns, no significance; * $p<0.05$; ** $p<0.01$; *** $p<0.001$; **** $p<0.0001$. The p-values were calculated using one-way ANOVA. E) Schematic of testing different combinations of cytokines and small molecules. F) The flow cytometric analysis of SOX17-positive cells. G) Bar chart showing the SOX17 positive cells quantified by flow cytometry analysis as in (F). The data are presented as the mean ± SD. n = 3. ns, no significance. The p-values were calculated using one-way ANOVA.

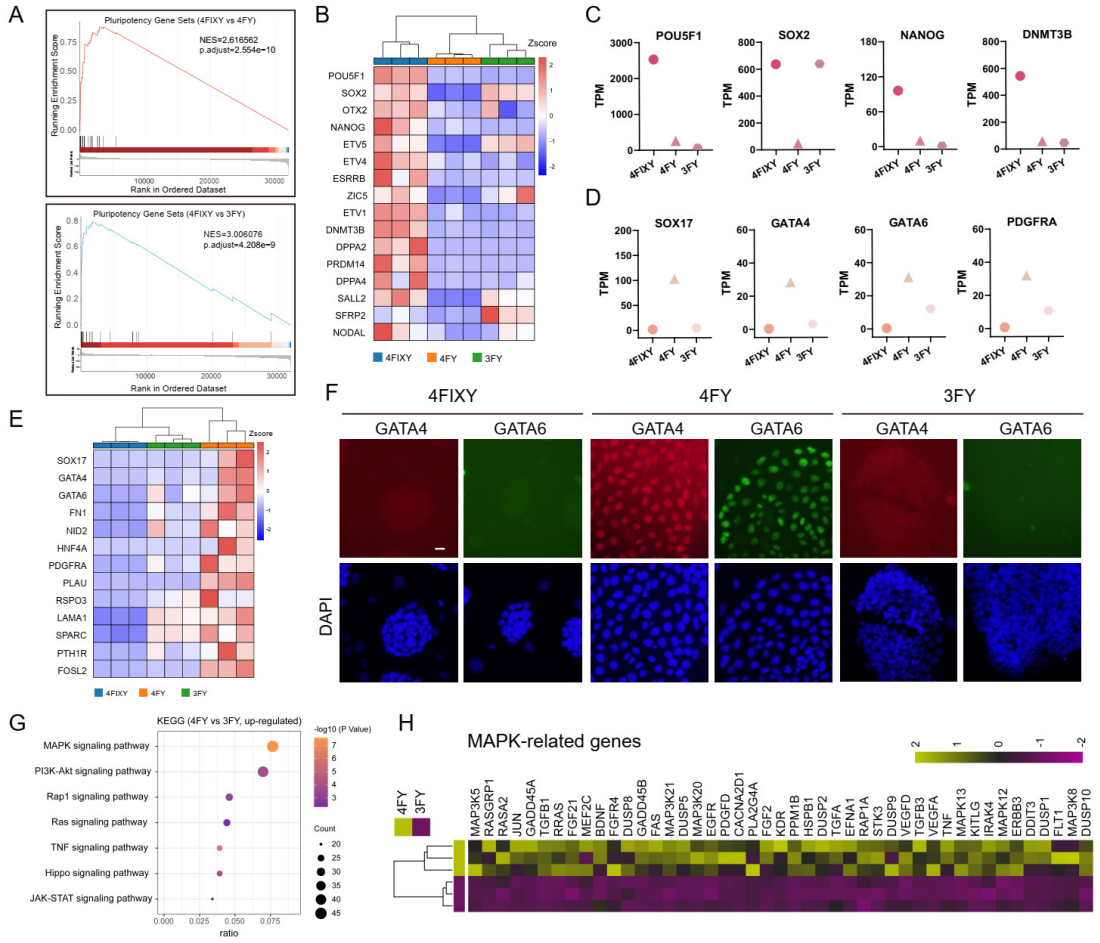


Figure S2. Removal of Activin A leads to failure in the conversion of XEN lineage. A) GSEA of pluripotency genes. B) Heatmap showing the expression of pluripotency genes. C) RNA-Seq expression (TPM values) of pluripotency genes. D) RNA-Seq expression (TPM values) of hypoblast/XEN genes. E) Heatmap showing the expression of hypoblast/XEN genes. F) Representative immunofluorescent staining for hypoblast/XEN markers. Scale bar, 20 µm. G) Top KEGG enrichment between 4FY and 3FY. H) Heatmap showing the expression of MAPK-related genes.

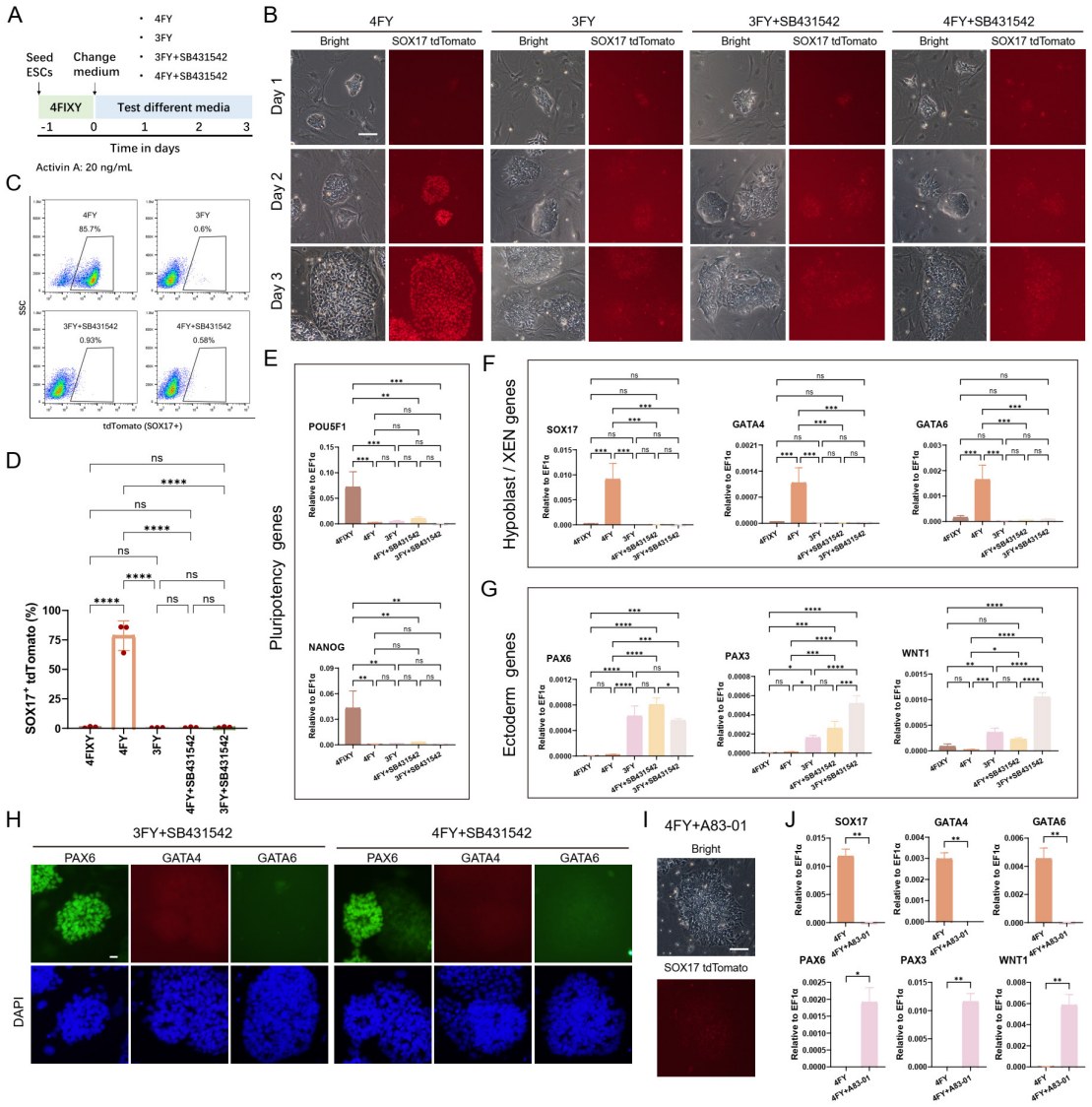


Figure S3. SB431542 inhibits Activin A-induced porcine ESC-to-XEN transition. A) Schematic of adding SB421542 in 4FY and 3FY during ESC-to-XEN cell transition. B) Morphology of cells in 4FY, 3FY, 4FY+SB431542, and 3FY+SB431542. Scale bar, 100 μm. C) The flow cytometric analysis of SOX17-positive cells. D) Bar chart showing the SOX17 positive cells quantified by flow cytometry analysis as in (C). The data are presented as the mean ± SD. n = 3. ns, no significance; **** $p<0.0001$. The p-values were calculated using one-way ANOVA. E), F), and G) Real-time quantitative PCR data of pluripotency markers (E), hypoblast/XEN markers (F), and ectoderm markers (G). The data are presented as the mean ± SD. n = 3. ns, no significance; * $p<0.05$; ** $p<0.01$; *** $p<0.001$; **** $p<0.0001$. The p-values were calculated using one-way ANOVA. H) Immunofluorescent staining for ectoderm markers PAX6. Scale bar, 20 μm. I) Morphology of cells in 4FY+A83-01. J) Real-time quantitative PCR data of markers in 4FY+A83-01. The data are presented as the mean ± SD. n = 3. * $p<0.05$; ** $p<0.01$. The p-values were calculated using Student's t.

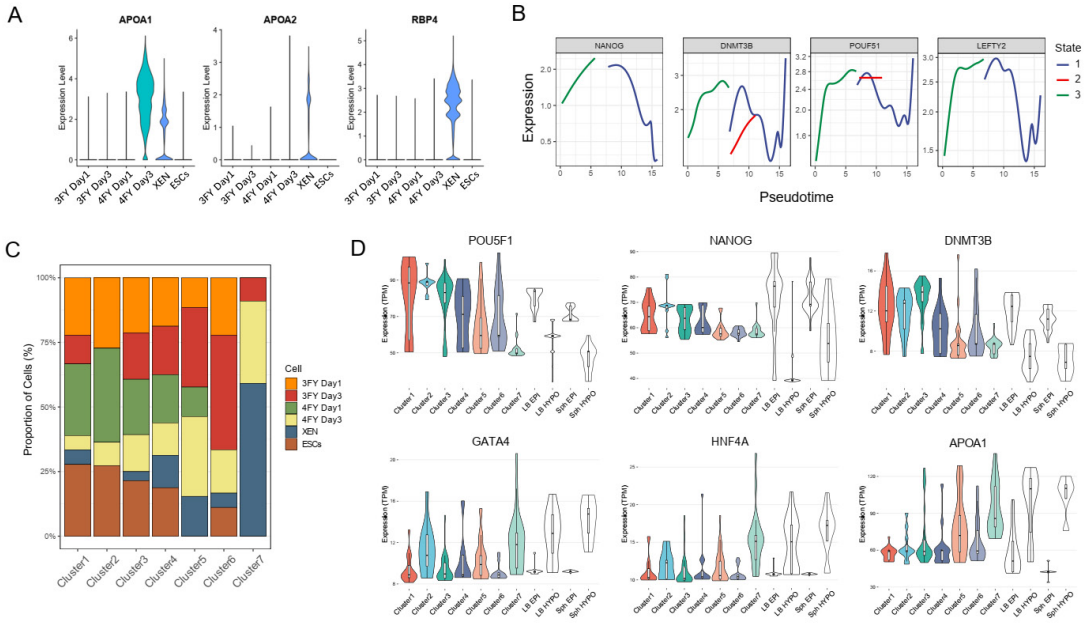


Figure S4. Gene expression based on the Single-cell analysis. A) Violin plots show markers highly expressed in the hypoblast, but lowly expressed in definitive endoderm in porcine embryos as in Simpson et al (2024) [1]. B) Expression of pluripotency genes as a function of pseudo-time. C) The cell proportion in individual cluster. D) Expression of pluripotency genes in each cluster and in vivo embryos[2]. LB: late blastocyst; Sph: spherical embryo; EPI: epiblast; HYPO: hypoblast.

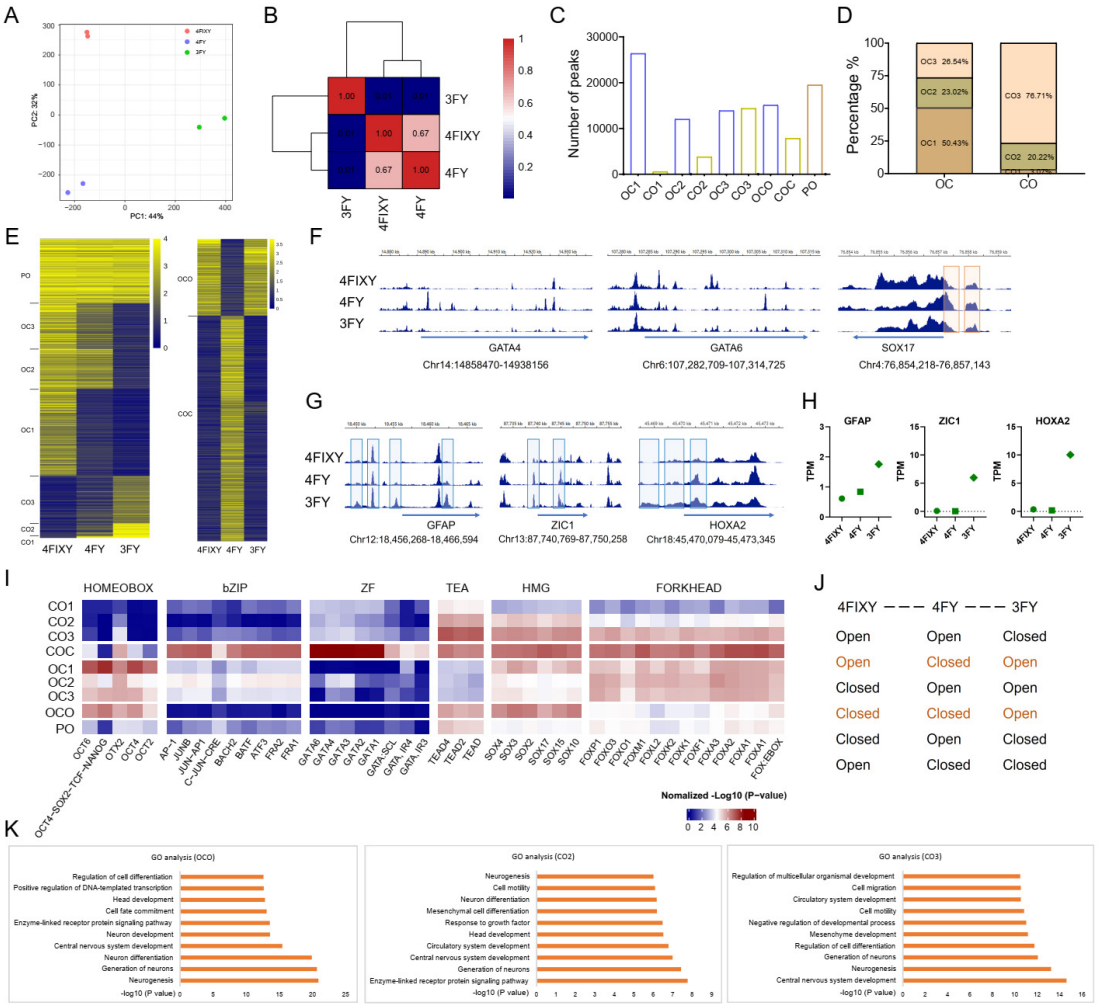


Figure S5. Chromatin accessibility dynamics in 3FY, 4FY, and 4FIXY cells. A) PCA analysis by ATAC-Seq data. B) Correlation analysis among 3FY, 4FIXY, and 4FY groups. C) The number of peaks defined as CO, OC, COC, OCO, and PO. D) The percentage of CO and OC peaks. E) The global CO, OC, COC, OCO, and PO status. F) Genome views of the ATAC-seq data for the hypoblast/XEN genes GATA4, GATA6, and SOX17. G) Genome views of the ATAC-seq data for the selected ectoderm genes. H) RNA-Seq analysis of the expression levels (TPM values) of the indicated genes. I) Heatmap showing the motif enrichment. TF families are indicated on the top. J) Schematic of GO enrichment of genes associated with open in 3FY and closed in 4FY peaks. K) GO analysis of genes related to OCO, CO2, and CO3 peaks.

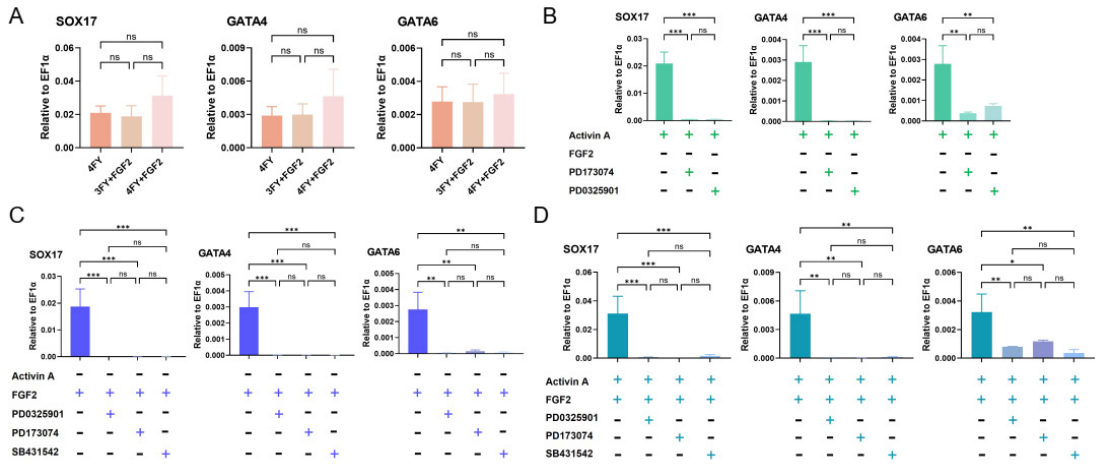


Figure S6. Hypoblast marker expression in varied culture systems. A) Real-time quantitative PCR data in 4FY, 3FY+FGF2, and 4FY+FGF2. The data are presented as the mean ± SD. n = 3. ns, no significance. B) Real-time quantitative PCR data in 4FY, 4FY+PD173074, and 4FY+PD0325901. The data are presented as the mean ± SD. n = 3. ns, no significance; ** $p<0.01$; *** $p<0.001$. The p-values were calculated using one-way ANOVA. C) Real-time quantitative PCR data in 3FY+FGF2, 3FY+FGF2+PD173074, 3FY+FGF2+PD0325901, and 3FY+FGF2+SB431542. The data are presented as the mean ± SD. n = 3. ns, no significance; ** $p<0.01$; *** $p<0.001$. The p-values were calculated using one-way ANOVA. D) Real-time quantitative PCR data in 4FY+FGF2, 4FY+FGF2+PD173074, 4FY+FGF2+PD0325901, and 4FY+FGF2+SB431542. The data are presented as the mean ± SD. n = 3. ns, no significance; ** $p<0.01$; *** $p<0.001$. The p-values were calculated using one-way ANOVA.

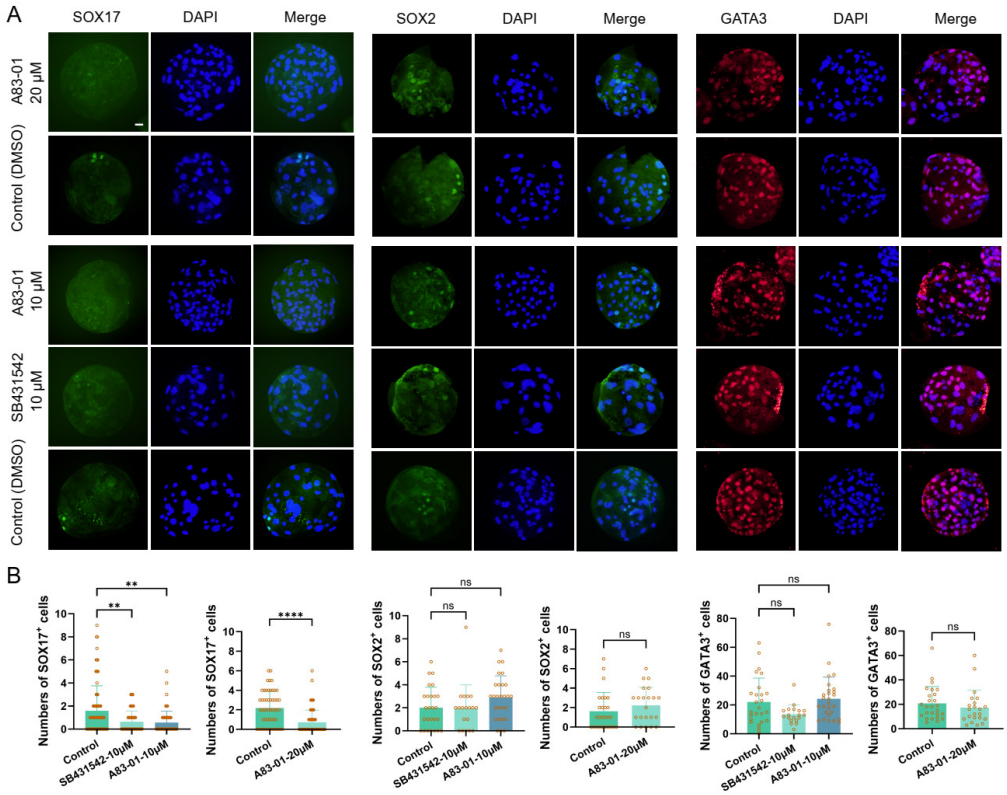


Figure S7. Immunofluorescence staining of porcine embryos. A) Immunofluorescence staining for SOX17, SOX2, and GATA3 in E6.5-7 blastocysts. B) Bar chart showing the number of hypoblast (SOX17-positive), epiblast (SOX2-positive), and trophectoderm (GATA3-positive) cells. Statistical tests: Kruskal-Wallis test with Dunn's multiple comparisons test. ns, no significance; * $p<0.05$; ** $p<0.01$; **** $p<0.0001$.

References

1. Simpson L, Strange A, Klisch D, Kraunsoe S, Azami T, Goszczynski D, et al. A single-cell atlas of pig gastrulation as a resource for comparative embryology. Nat Commun. 2024; 15.

2. Ramos-Ibeas P, Sang F, Zhu QF, Tang WWC, Withey S, Klisch D, et al. Pluripotency and X chromosome dynamics revealed in pig pre-gastrulating embryos by single cell analysis. Nat Commun. 2019; 10: 500.